Clinical and Experimental HEPATOLOGY

Clin Exp HEPATOL 2022; 8, 1: 60–69
DOI: https://doi.org/10.5114/ceh.2022.114192
Received: 30.11.2021, **Accepted:** 3.01.2022, **Published:** 23.03.2022

Original paper

Comparison of growth features and cancer stem cell prevalence in intrahepatic and extrahepatic cholangiocarcinoma cell lines

Jiaqi Yang[1], David P. Sontag[1], Frank J. Burczynski[1], Shengyan Xi[2], Yuewen Gong[1], Gerald Y. Minuk[1]

[1]University of Manitoba, Canada
[2]Xiamen University, China

Abstract

Aim of the study: Intra- and extrahepatic cholangiocarcinoma (I-CCA and E-CCA respectively) exhibit different growth features that contribute to different clinical outcomes. Cancer stem cells (CSCs) influence tumor growth and thereby may be responsible for these differences. The aim of this study was to document and compare the growth features of human I-CCA and E-CCA cell lines and determine whether any differences observed could be explained by differences in the prevalence and/or stem cell surface marker (SCSM) expression profiles of CSCs within the tumor cell lines.

Material and methods: Six CCA cells lines, three I-CCA and three E-CCA, were studied. Tumor cell growth features including cell proliferation, colony/spheroid formation, migration and invasion were documented. CSC prevalence and SCSM expression profiles were examined by flow cytometry.

Results: I-CCA cells had significantly increased proliferative activity, shorter doubling times and were more invasive than E-CCA cells, while colony/spheroid formation and migration were similar in the two cell populations. There were no significant differences in CSC prevalence rates or SCSM expression profiles.

Conclusions: These findings suggest that I-CCA cells proliferate at a more rapid rate and are more invasive than E-CCA cells but the differences cannot be explained by differences in the prevalence or SCSM expression profiles of CSCs within the tumor cell population.

Key words: cholangiocarcinoma, stem cell markers, stem cell features, intrahepatic, extrahepatic.

Address for correspondence

Dr. Gerald Yosel Minuk, University of Manitoba, Canada, e-mail: gerald.minuk@umanitoba.ca

Introduction

Cholangiocarcinoma (CCA) is a rare but often fatal cancer of the liver [1]. It can be classified as either intrahepatic (I-CCA) or extrahepatic (E-CCA) depending on its anatomical location. Despite the fact both tumor subtypes consist of malignant cholangiocytes, distinct differences exist in their respective growth patterns and clinical courses [2, 3]. For example, I-CCA grow rapidly, form masses, are invasive, and often metastasize. On the other hand, E-CCA grow slowly, along tissue planes of adjacent structures, are less invasive and only rarely develop distant metastases [4, 5]. These differences could be explained by differences in tumor cell biology and/or the prevalence and stem cell surface marker (SCSM) expression profiles of cancer stem cells (CSCs) within the tumor cell population.

Cancer stem cells are a subpopulation of tumor cells that have the ability to self-replicate and differentiate into different cell lineages [6]. They can be identified by the expression of certain SCSMs including CD13 [7], CD24 [8], CD44 [9, 10], CD90, CD133 and epithelial cell adhesion molecule (EpCAM) [11, 12]. CSCs are thought to be responsible for tumor initiation, growth, migration, invasion and metastasis, and each SCSM has been associated with specific tumor cell features [13, 14].

In the current study, we documented and compared I-CCA and E-CCA tumor cell growth features and attempted to determine whether any differences that might exist could be explained by differences in CSC prevalence and/or SCSM expression within the various tumor cell populations.

Material and methods

Cell lines

The HuCCT-1 cell line was purchased from Sekisui XenoTech (USA) and KMBCs from ATCC (USA). The remaining cell lines CCLP-1, SG231, HuH28, TFK-1 and H69 were obtained from Dr. Gianfranco Alpini at Texas A&M University. HuCCT-1, CCLP-1 and SG231 are derived from I-CCAs while KMBC, HuH28 and TFK-1 originate from E-CCAs [15, 16]. H69 cells are transformed bile duct epithelial cells and are derived from normal cholangiocytes [17]. This study was approved by the University of Manitoba Conjoint Ethics Committee for Human and Animal Experimentation.

Reagents

RPMI 1640, Dulbecco's Modified Eagle Medium (DMEM), Minimum Essential Media (MEM), trypsin-EDTA and fetal bovine serum (FBS) were obtained from Invitrogen (USA). APC-conjugated anti-human CD13 monoclonal antibodies (mAbs) (BD Biosciences, USA), APC-eFluor 780-conjugated anti-human CD24 mAb (Life technologies, USA), eFluor 450-conjuagted anti-human CD44 mAb (Life Technologies, USA), PE-Cy7 conjugated anti-CD90 mAb (BD Biosciences, USA), PE-conjugated CD133 mAb (Miltenyi Biotec, USA), FITC-conjugated anti-human EpCAM mAb (Miltenyi Biotec, USA), and cell viability marker 7-AAD (Beckman Coulter, USA) were applied for flow cytometry. Fluorescence conjugated isotype-matched antibodies were purchased from Life Technologies, BD Biosciences, Santa Cruz and Miltenyi Biotec (USA).

Cell culture

HuCCT1, HuH28, KMBC, and TFK-1 cells were cultured in RPMI 1640 medium supplemented with 110 mg/l sodium pyruvate, 10% HI-FBS, 100 U/ml penicillin and 100 µg/ml streptomycin (Invitrogen, USA). CCLP-1 cells were cultured in DMEM, supplemented with 10% FBS, 2 mmol/l L-glutamine, 100 U/ml penicillin and 100 µg/ml streptomycin. SG231 cells were cultured in MEM, supplemented with 10% FBS, 2 mmol/l L-glutamine, 25 mM HEPES pH 7.2, and 100 U/ml penicillin and 100 µg/ml streptomycin [15, 16]. H69 cells were cultured in DMEM (low glucose, Gibco), 25% Ham's F12, 10% FBS, 4 mmol/l L-glutamine, 180 µmol/l adenine, 5 mg/l insulin, 5 mg/l transferrin, 2 nmol/l triiodothyronine, 1.1 µmol/l hydrocortisone, 5.5 µmol/l epinephrine, 1.64 µmol/l epidermal growth factor (EGF), 100 U/ml penicillin and 100 µg/ml streptomycin. All cells were incubated at 37°C in a humidified atmosphere of 5% CO_2 and 95% air [17].

Cell proliferation

Cell proliferation and doubling times were determined by seeding CCA cells at a density of 2000 cells per well in 96-well plates. The number of cells in each well was counted on days 0, 1, 3 and 6 after plating by adding a cell proliferation indicator: premixed WST-1 reagent (Takara Bro, USA) and incubating at 37°C for 3 hours as described [12]. The absorbance of each well against a blank control was measured using a microplate reader (Synergy 4, Biotek, Wi, USA) at 540 nm. Cell doubling times were calculated using the equation:

$$\text{Doubling time} = \textit{duration} \times \frac{\textit{log}\,(2)}{\textit{log (final absorbency)} - \textit{log (initial absorbency)}}$$

where duration = day 6 – day 3 (72 hours), final absorbency: absorbency of day 6, initial absorbency: absorbency of day 3.

Colony formation

The tumorigenic capacity of sorted cells was tested by the soft agar colony formation assay as described previously [18]. CCA cells were seeded on a dual-layer soft agar. The bottom layer was composed of a 0.75 ml mixture of 1% Nobel agar and 2× corresponding completed medium (1 : 1), and the top layer of a 0.75 ml mixture of 0.6% Nobel agar and 2× corresponding completed medium. The top layer contained approximately 5,000 sorted cells (1 : 1). Plates were incubated for 21 days in a 37°C incubator. Each well was stained with 300 µl of 10 mg/ml p-Nitroblue tetrazolium chloride and incubated at 37°C overnight. Photographs of wells containing stained colonies were analyzed using ImageJ software with the ColonyArea plugin [19]. The colony intensity is calculated by [19]:

$$\text{Colony intensity \%} = \frac{\sum \textit{pixel intensities in a region}}{\sum \textit{maximum intensitites possible in the same region}} \times 100$$

Spheroid formation

Cells were trypsinized and resuspended in DMEM/F12 medium, supplemented with 1 × B-27 serum-free

supplement, 4 μg/ml heparin, 100 U/ml penicillin, 100 μg/ml streptomycin, 10 ng/ml EGF, and 10 ng/ml bFGF [12]. Cells were subsequently seeded at densities of 200 cells per well in ultra-low attachment 96-well plates. After 0, 3 and 6 days of culture, spheroids were photographed under the microscope. Aggregation diameters were measured and analyzed by ImageJ software.

Wound healing

Cells (0.5×10^6/ml, 2 ml per well) were seeded in 6-well plates and cultured with culture medium with 10% FBS until confluent. Cell monolayers were scratched with a 200 μl pipette tip to generate a wound according to the method described previously [12]. Phase contrast images were taken at initiation of the wound for different cells and captured again after 6, 12, 18, 24, 30, 36, 42, 48, 60, 72 and 84 hours until the closure was completed. Images acquired were analyzed quantitatively using ImageJ software. By comparing the images from each captured time point, the migration capacity of cells was measured as the extent of wound closure (gap) by calculating wound area. The half-closure time was calculated using the formula:

$$T_{1/2}\text{gap} = \frac{\textit{initial gap area}}{\textit{2 x slope}}$$

Gap area was measured and plotted as a function of time. Complete closure was considered the time point at which the wound was completely closed.

Invasion

Twenty-four well Transwell permeable chambers with 8 μm pores (Corning, USA) were used to measure cell invasion. To the upper chambers, 1×10^5 cells were added in 100 μl of corresponding serum-free medium. Lower chambers were filled with 650 μl of medium and 10% FBS. After 24 hours of incubation, cells from the upper surface were removed with cotton swabs. Penetrated cells were dissociated and collected by a cell dissociation buffer (Invitrogen, USA) as described previously [20]. Collected cells were counted by a cell counter (Cellometer Auto 2000, Nexcelom Bioscience, USA).

CSC and SCSM identification by flow cytometry

Cells were cultured in a 35 cm culture dish until 75% confluence, and then trypsinized and resuspended in phosphate-buffered saline (PBS) with 1.5% FBS, 25 mM HEPES pH 7.0, and 1 mM EDTA (Sigma-Aldrich, USA). Cells were then transferred into 75 mm polystyrene round-bottom test tubes (BD Falcon, USA) at a concentration of 1×10^6 cells/ml, stained with fluorescence-conjugated antibodies (anti-CD13-APC, anti-CD24-APC-eFlour 780, anti-CD44-eFluor 450, anti-CD133-PE, anti-EpCAM-FITC, and 7-AAD) as previously described [12]. Cells stained with isotype-matched antibodies (BD Biosciences, USA) served as negative controls. Flow cytometer analysis was performed on a BD FACSCanto-II Digital Flow Cytometry Analyzer (USA) using FlowJo (Tree Star, USA) software.

Statistical analysis

All experiments were performed in triplicate and repeated on a minimum of three occasions. Significant differences were determined by repeated measures of ANOVA and/or Tukey's multiple comparison post-hoc test. Student's *t*-test was used for comparisons of two groups. A significant correlation was demonstrated by the Pearson correlation coefficient test. Data were analyzed by GraphPad Prism 6 statistical software (GraphPad Software, Inc., USA). Differences with p values below 0.05 were considered statistically significant.

Results

Proliferation

The proliferative activities of the three I-CCA, three E-CCA and one non-malignant H69 cholangiocyte cell lines were determined by the WST-1 assay. The results are shown in Figure 1. The mean proliferation rates of I-CCA cells were similar to those of E-CCA cells until day 6, when they were significantly higher in I-CCA cells (3.49 ±0.51 vs. 2.35 ±0.58, $p < 0.05$). In addition, the overall doubling time for I-CCA cells was significantly shorter in I-CCA (39.9 ±2.6 hours) versus E-CCA (54.6 ±9.1 hours) cells ($p < 0.01$). The doubling time of non-malignant H69 cholangiocytes was intermediate between I-CCA and E-CCA cells (47.3 ±8.9 hours).

Colony formation

The results of colony formation in soft-agar gels are shown in Figure 2. There were no significant differences in the colony intensities of I-CCA and E-CCA cell lines (51.3 ±7.4% vs. 45.9 ±20.1%, respectively, $p = 0.46$). The colony intensity of non-malignant H69 cholangiocytes was somewhat higher (63.0 ±4.97%) but not significantly different from that of I-CCA or E-CCA cell lines.

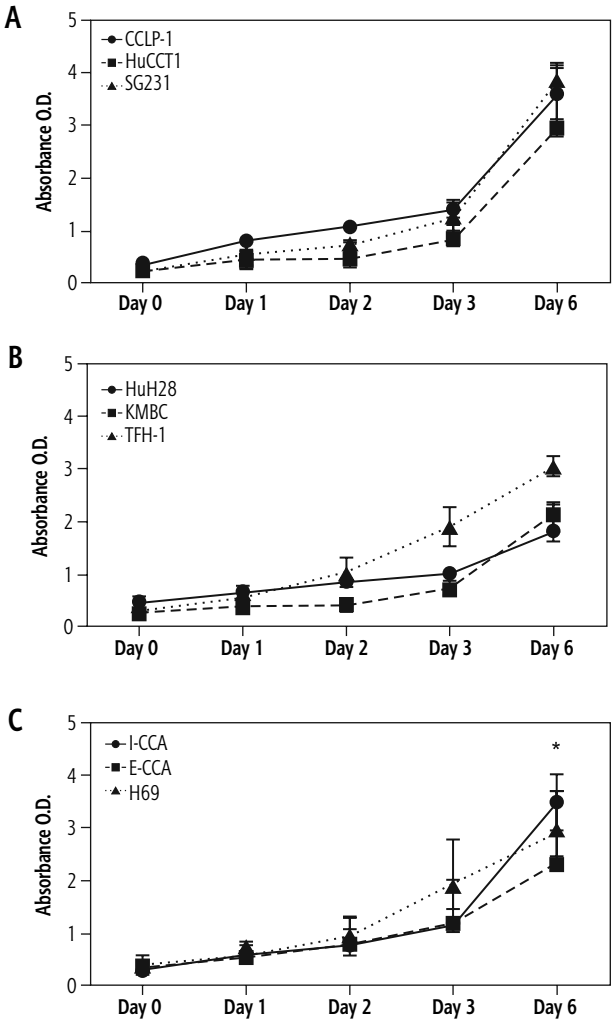

I-CCA cell lines	Doubling time (h)
CCLP-1	44.4 ±2.7
HuCCT1	39.7 ±3.6
SG231	35.4 ±1.9

E-CCA cell lines	Doubling time (h)
HuH28	72.6 ±6.4
KMBC	48.2 ±3.5
TFK-1	43.1 ±1.3

Cell lines	Doubling time (h)
I-CCA	39.9 ±2.6**
E-CCA	54.6 ±9.1
Non-malignant	47.3 ±8.9

Fig. 1. Proliferative activity of individual/aggregated I-CCA, E-CCA and non-malignant H69 cholangiocyte cell lines. Five thousand cells of each cell line were cultured for 1, 2, 3, and 6 days. Proliferative activity was significantly higher in aggregated I-CCA vs. E-CCA cell lines on day 6 and overall doubling times were shorter in aggregated I-CCA vs. E-CCA cell lines. Data presented as the mean ±SD from a minimum of three experiments. *$p < 0.05$, **$p < 0.01$ I-CCA vs. E-CCA

Spheroid formation

The mechanism responsible for spheroid formation in I-CCA and E-CCA cells was somewhat different in that I-CCA cells tended to develop spheroids as a result of single cell proliferative activity, whereas in E-CCA cells the process predominantly consisted of the aggregation of multiple cells. Nonetheless, the mean diameters of I-CCA and E-CCA spheroids at day 6 were similar (137 ±32.1 μm and 144 ±31.0 μm respectively, $p = 0.40$) and significantly smaller than those observed with non-malignant H69 cholangiocytes (177 ±15.8 μm, $p < 0.001$ and 0.01, respectively) (Fig. 3).

Migration

Figure 4 provides representative photographs of wound healing assays at three time points: 0, 12 and 24 hours for I-CCA, E-CCA and non-malignant H69 cholangiocytes. There was significant cell line specific heterogeneity. Specifically, SG231 I-CCA cells exhibited delayed wound closure compared to CCLP-1 and HuCCT1 cells, whereas for E-CCA cells, TFK-1 closure was significantly delayed relative to HuH28 and KMBC cells. However, the mean aggregated times to one half wound closure (17.0 ±10.3 hours for I-CCA and 24.4 ±11.8 hours for E-CCA cell lines) were similar ($p = 0.179$), as were the times to complete wound closure (38.0 ±29.6 vs. 50.0 ±30.8 hours respectively, $p = 0.652$). One half and complete wound closure times for non-malignant H69 cholangiocytes (20.8 ±2.5 and 42.0 ±0.0 hours respectively) were similar to those observed in I-CCA and E-CCA cell lines.

Invasion

Figure 5 illustrates the results of cell invasion experiments for I-CCA, E-CCA and non-malignant H69

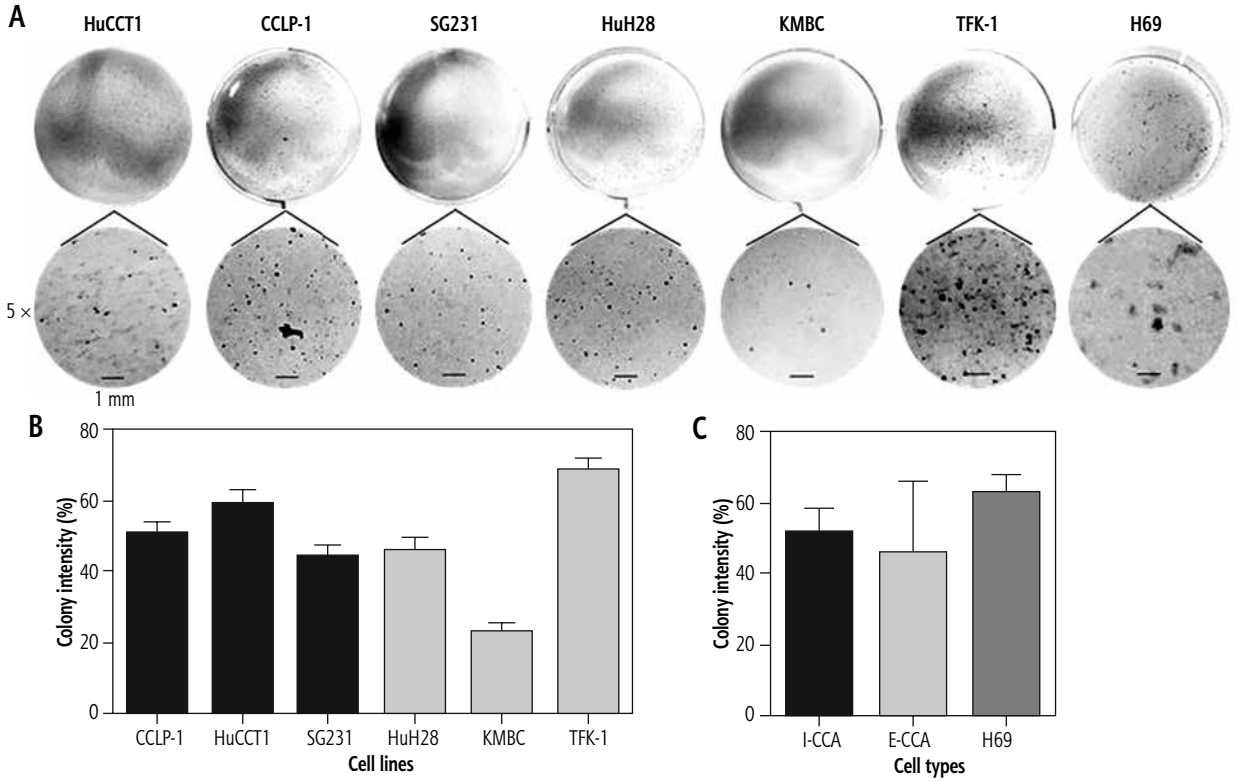

Fig. 2. Colony formation of individual/aggregated I-CCA, E-CCA and non-malignant H69 cholangiocyte cell lines. **A**) Soft-agar colony formation in each cell line after 21 days of incubation. The lower panels are 5× the optical zoom of corresponding soft agar plates. **B, C**) Quantification of colony intensity for individual cell lines and aggregates of I-CCA and E-CCA cell lines by ImageJ analysis. Data presented as the mean ±SD from a minimum of three experiments. Scale bar: 1 mm

cholangiocyte cell lines. In general, I-CCA cell lines invaded Transwell chambers to a greater extent than E-CCA cell lines (cell numbers: 4,466 ±1,531 vs. 2,692 ±1,030, $p < 0.05$). Both tumor cell lines invaded to a greater extent than non-malignant H69 cholangiocytes (562 ±78.9, $p < 0.001$ and 0.05, respectively).

CSC prevalence and SCSM expression

By employing flow cytometry, the prevalence and distribution of SCSMs – CD13, CD24, CD44, CD90, CD133 and EpCAM – were documented (Fig. 6). Among the six CCA cell lines, HuCCT1 cells appeared to have the highest expression of all six stem cell surface markers, while few KMBC cells expressed these markers other than CD90, which was expressed by 53% of KMBC cells. Other cell lines expressed intermediate prevalence of cell surface markers. Overall, there were no significant differences in the prevalence of CSCs or SCSMs between I-CCA and E-CCA cell lines. Almost all non-malignant H69 cholangiocytes expressed CD13 and CD90.

To determine whether SCSMs were consistently expressed (a feature of stem cell replication), cells were cultured for 30 days and marker expression documented at the end of the culture period. As shown in Table 1, there were no significant changes in SCSMs over the 30 day period.

Finally, to determine whether specific SCSMs associate with certain tumor cell growth features, correlation coefficients were calculated for each stem cell marker and cell proliferation, colony/spheroid formation, migration and invasion assays. The results (Table 2) revealed no significant correlations between specific SCSMs and cell growth properties.

Discussion

The results of this study suggest that I-CCA cells proliferate more rapidly and are more invasive than E-CCA cells. However, other tumor cell growth features such as colony/spheroid formation and cell migration were similar in the two cell populations. The results also suggest that differences in cell proliferative activity and invasion cannot be explained by differences in the prevalence and/or SCSM expression profiles of CSCs within the tumor cell populations. Overall, the results support the concept that at least some of the clinical differences in I-CCA and E-CCA growth reflect inherent differences in the two cell populations, but others likely reflect differences in their respective tumor microenvironments.

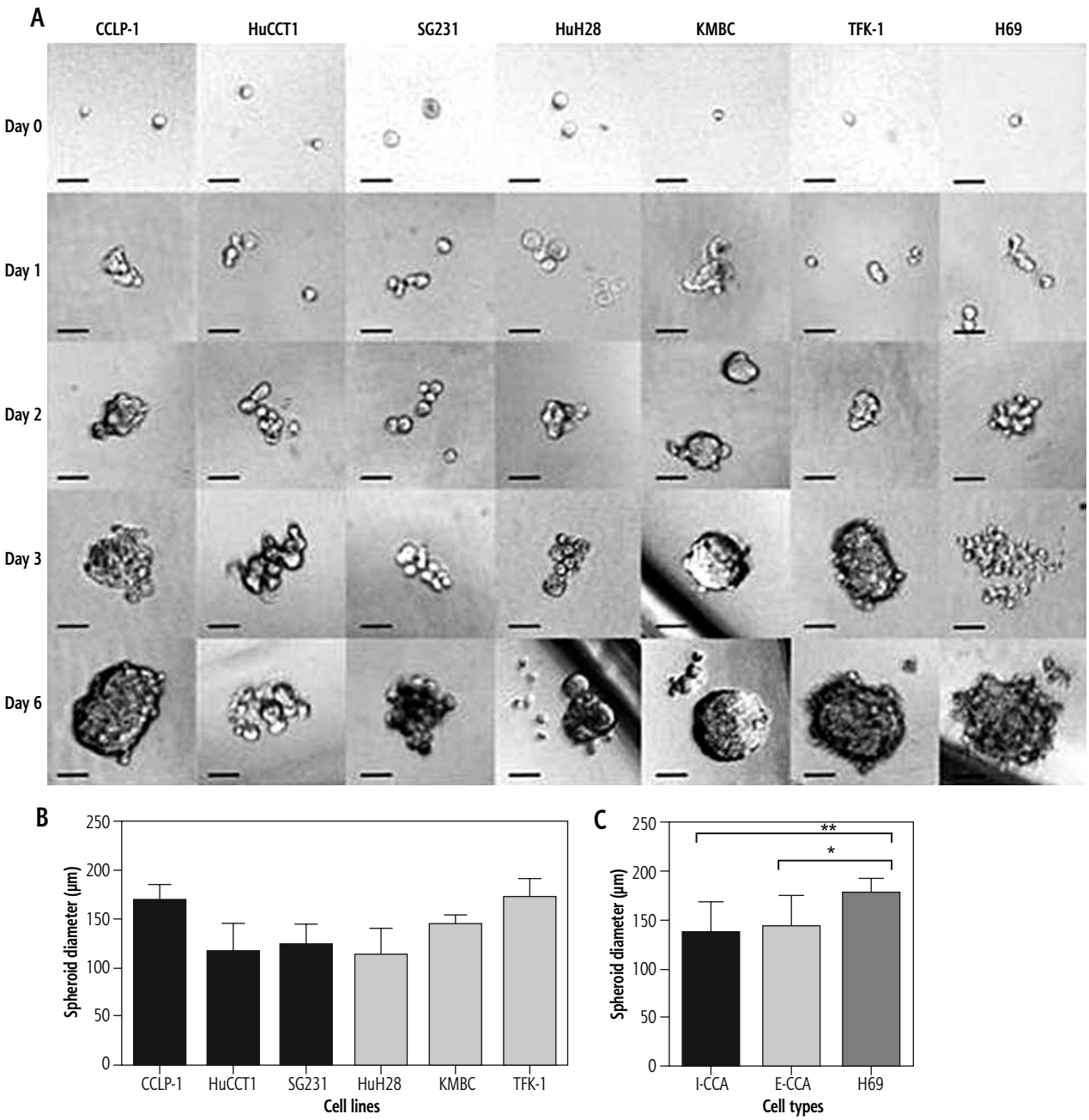

Fig. 3. Spheroid formation of individual/aggregated I-CCA, E-CCA and non-malignant H69 cholangiocyte cell lines. Cells were seeded at densities of 2000 cells/well in ultra-low 96-well plates to generate spheroids. **A**) Spheroid formation from days 0 to 6. **B, C**) Spheroid diameters documented by ImageJ analysis. Data presented as the mean ±SD from a minimum of three experiments. Scale bar: 50 µm. *$p < 0.01$, **$p < 0.001$

Numerous previous clinical studies have documented significant differences in I-CCA and E-CCA growth patterns (reviewed in ref. [2]). Specifically, I-CCAs form masses with well demarcated (add space between words) demarcated nodules that grow in a radial pattern. They tend to invade the local microvasculature and develop distant metastases. Microscopically, ductular morphology with mucin production or features of hepatocellular differentiation may be present. E-CCAs on the other hand tend to be sclerosing or polypoid and non-mucin producing [4, 21]. They tend to grow within bile duct lumens, along the bile duct wall or parallel to adjacent tissue planes and tend not to invade or metastasize. In addition, the derivation of I-CCA and E-CCA may differ in that I-CCAs are thought to be derived from the malignant transformation of hepatic stem cells [22, 23], whereas E-CCAs develop as a result of epithelial to mesenchymal transformation of ductular cholangiocytes [21].

Cancer stem cells are a subpopulation of cells that influence tumor growth and progression [6]. Previous stud-

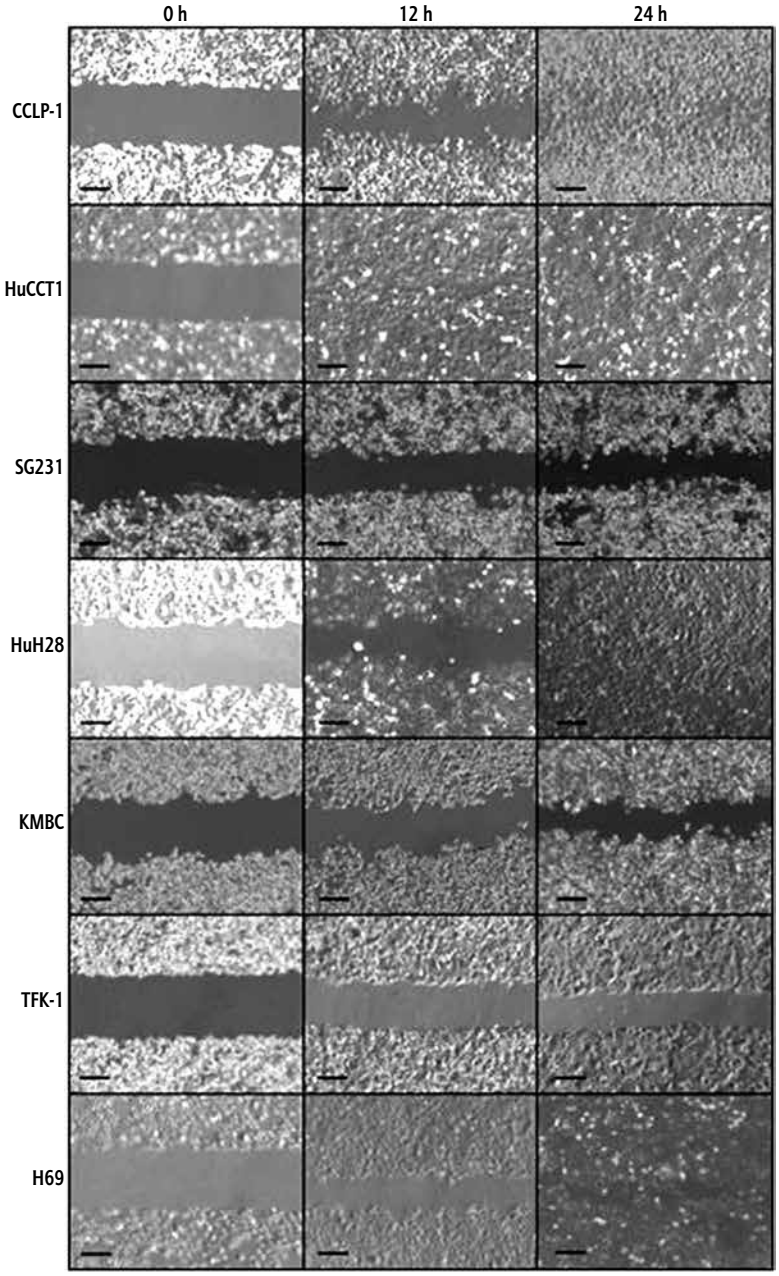

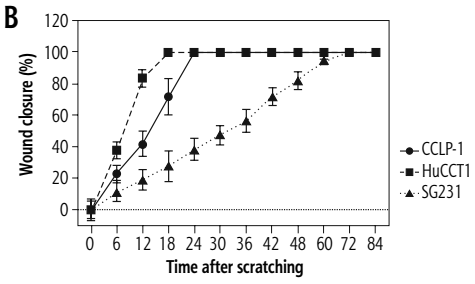

I-CCA cells	$T_{1/2}$gap (h)
CCLP-1	13.2 ±1.9
HuCCT1	7.68 ±1.35
SG231	30.1 ±3.5

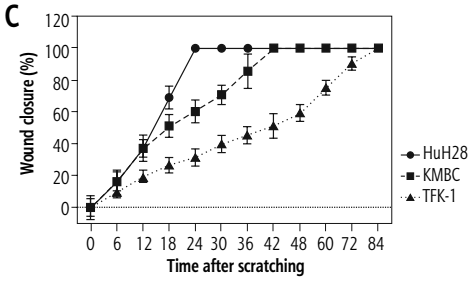

E-CCA cells	$T_{1/2}$gap (h)
HuH28	14.9 ±1.8
KMBC	18.5 ±2.6
TFK-1	39.7 ±3.3

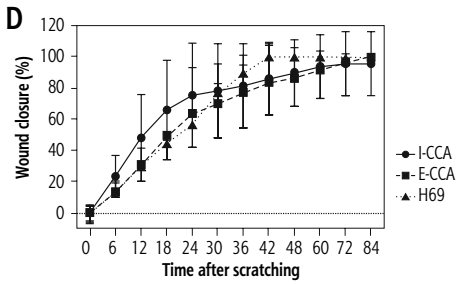

Cell lines	$T_{1/2}$gap (h)
I-CCA	17.0 ±10.3
E-CCA	24.4 ±11.8
Non-malignant	20.8 ±2.5

Cell lines	Wound complete (h)
I-CCA	38 ±29.6
E-CCA	50 ±30.8
Non-malignant	42 ±0

Fig. 4. Wound healing assay of individual/aggregated I-CCA, E-CCA and non-malignant H69 cholangiocyte cell lines. **A**) Phase contrast of cell migration photographed at 0, 12, and 24 hours after scratching. **B-D**) ImageJ analysis of cell migration by measuring area closure from phase-contrast images. $T_{1/2}$gap: time for wound to close to 50% of original area. Data presented as the mean ±SD from a minimum of three experiments. Scale bar: 250 µm

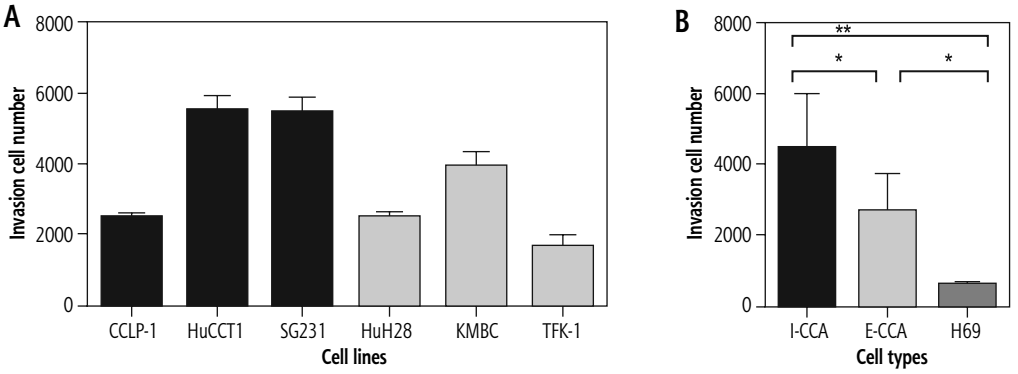

Fig. 5. Transwell invasion of individual/aggregated I-CCA, E-CCA and non-malignant H69 cholangiocyte cell lines after 24 hours of incubation. Data presented as the mean ±SD from a minimum of three experiments. *$p < 0.05$, **$p < 0.001$

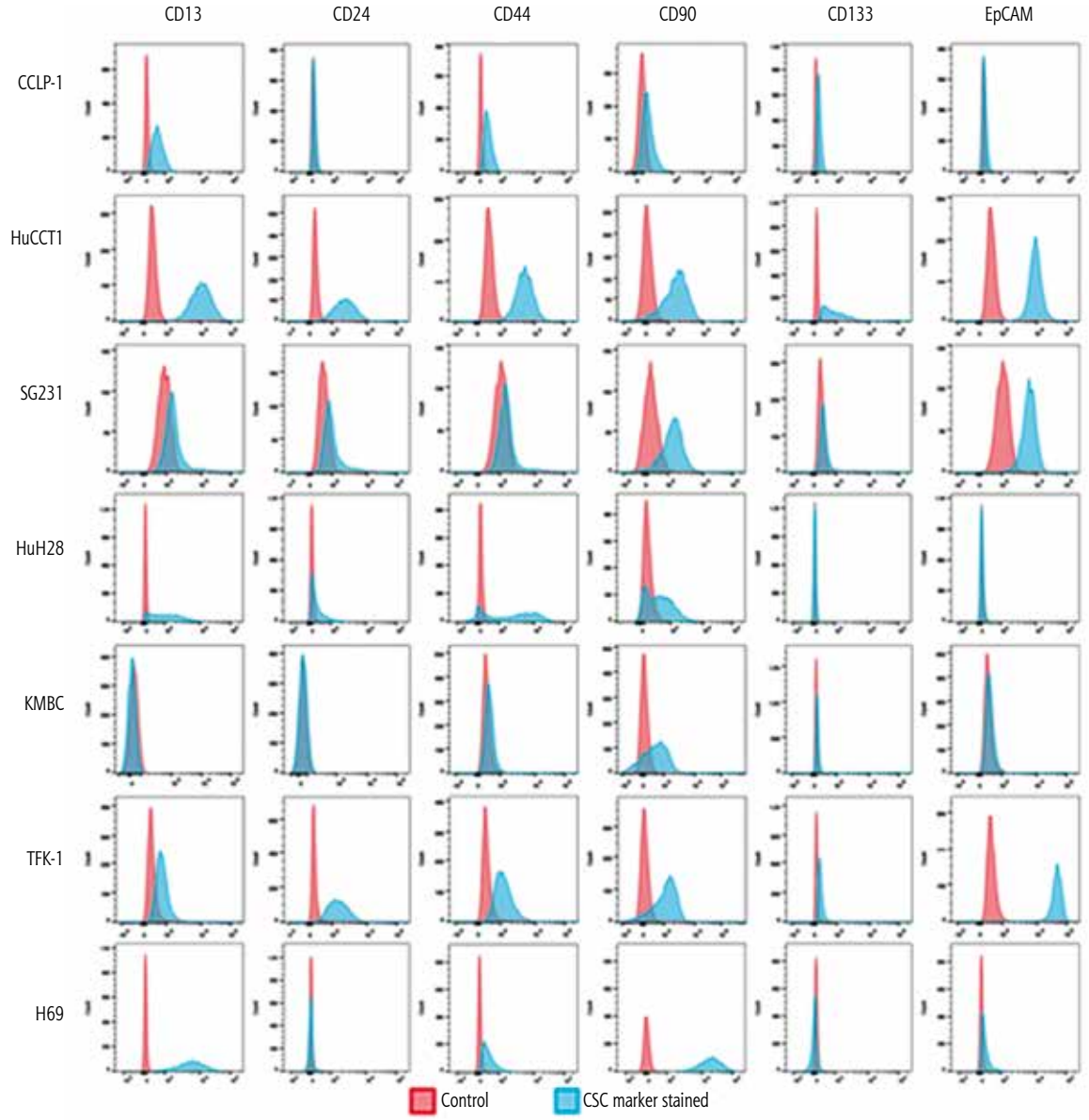

Cell lines		CSC marker expression (%)					
		CD13	CD24	CD44	CD90	CD133	EpCAM
I-CCA	CCLP-1	61.7 ±4.5	3.41 ±1.16	35.1 ±5.8	11.2 ±1.8	9.17 ±2.90	2.21 ±1.06
	HuCCT1	100 ±0.06	97.2 ±1.1	97.8 ±2.8	80.4 ±3.57	90.7 ±1.9	99.9 ±0.01
	SG231	11.8 ±1.3	16.1 ±2.9	8.27 ±2.43	48.0 ±3.87	9.74 ±0.84	99.0 ±0.5
E-CCA	HuH28	88.3 ±2.2	46.2 ±3.3	90.8 ±1.4	68.6 ±6.61	2.49 ±1.40	0.35 ±0.47
	KMBC	0.67 ±0.54	0.99 ±0.06	3.96 ±1.64	52.8 ±2.81	0.45 ±0.13	0.92 ±0.30
	TFK-1	18.2 ±9.7	97.2 ±3.7	58.0 ±3.4	81.5 ±4.50	2.45 ±1.40	99.3 ±1.0
Non-malignant	H69	99.1 ±0.7	1.16 ±0.53	31.4 ±2.1	100 ±0.06	0.61 ±0.26	8.23 ±1.17

Fig. 6. Expression of stem cell surface markers (SCSMs) in cancer stem cell (CSC) in I-CCA (CCLP-1, HuCCT1, SG231), E-CCA (HuH28, KMBC, TFK-1) and non-malignant H69 cholangiocyte cell lines. Cells were stained with isotype-matched mABs (IgG1) or fluorescence-conjugated mAbs against CD13, CD24, CD44, CD90, CD133, and EpCAM and analyzed by flow cytometry. **A**) Cells stained with IgG1 (control/red color) and mAbs against the SCSM (blue color). **B**) Prevalence of SCSM positive population in each cell line. Data presented as the mean ±SD from triplicate experiments

Table 1. Stem cell surface marker expression in I-CCA and E-CCA cells after 30 days in culture

Cell lines		Marker expression											
		CD13		CD24		CD44		CD90		CD133		EpCAM	
		Day 1	Day 30	Day 1	Day 30	Day 1	Day 30	Day 1	Day 30	Day 1	Day 30	Day 1	Day 30
I-CCA	CCLP-1	61.0 ±2.45	67.9 ±3.32	1.94 ±0.61	4.38 ±1.79	33.1 ±5.25	32.8 ±1.85	10.7 ±2.25	12.1 ±1.1	10.2 ±2.16	8.59 ±0.88	1 ±0.10	2.46 ±1.29
	HuCCT1	99.6 ±0.25	99.8 ±0.29	96.3 ±3.26	98.1 ±3.12	96.6 ±2.68	98.5 ±1.77	88.1 ±2.84	85.1 ±5.06	91.7 ±1.10	91.0 ±3.37	99.9 ±0.06	99.9 ±0.12
	SG231	11.8 ±1.06	11.1 ±1.37	16.9 ±3.40	19.1 ±1.35	9.31 ±1.49	8.36 ±1.99	51.0 ±3.01	51.2 ±2.37	8.41 ±1.93	9.89 ±1.74	99.9 ±0.12	99.4 ±0.78
E-CCA	HuH28	89.3 ±3.40	90.8 ±2.26	44.4 ±3.32	46.7 ±3.88	89.8 ±3.86	89.1 ±4.60	68.8 ±3.05	68.6 ±4.15	4.23 ±0.78	1.92 ±0.88	0.36 ±0.45	0.63 ±0.28
	KMBC	1.73 ±1.15	0.93 ±0.66	0.44 ±0.43	1.35 ±0.32	2.75 ±1.34	3.60 ±0.94	49.9 ±1.42	49.0 ±3.50	0.34 ±0.29	0.51 ±0.43	0.68 ±0.38	0.99 ±0.29
	TFK-1	19.6 ±2.34	20.0 ± 2.98	97.3 ±3.38	96.2 ±1.51	56.4 ±1.64	60.1 ±2.36	81.1 ±3.04	80.8 ±2.35	2.40 ±1.35	2.26 ±1.46	99.6 ±0.55	99.3 ±0.64

Data present as the mean ± SD.

ies have documented adverse clinical outcomes in patients with high CSC prevalence [24]. In CCA, Cardinale *et al*. reported that more than 30% of the human CCA tumor mass consists of CSCs [25]. In the present study, at least one SCSM was expressed in the majority of I-CCA and E-CCA cell lines. However, there was much heterogeneity. For example, 99% of SG231 (I-CCA) cells were EpCAM positive and 48% CD90 positive, while other markers were present in less than 20% of SG231 cells. In HuH28 (E-CCA) cells, 91% expressed CD44, 88% CD13, 69% CD90, 46% CD24, while less than 2% were CD133 and EpCAM positive. Notwithstanding these differences, there was no clear suggestion that I-CCA and E-CCA cell lines had increased (or decreased) CSC prevalence or a predominance of specific SCSMs. Moreover, there were no associations between these SCSMs and tumor cell growth features.

Taken together, the results of this study suggest that both intrinsic differences in cell biology and the influence of the tumor microenvironment are more responsible for determining tumor growth patterns than the prevalence/SCSM expression profiles of CSCs within the tumor. Of note, the specific component(s) of the tumor microenvironment which may include the extracellular matrix, chemokines, bile salts, and neuropeptides have yet to be identified [26, 27].

There are a number of limitations to this study that warrant emphasis. First, although the cell lines studied were designated I-CCA or E-CCA by their sources [16, 28], controversy exists regarding such classifications, particularly for cells derived from tumors within the hilar region of the liver. This concern is underscored by the uncertainty of the derivation of HuH28 cells, which have been considered I-CCA by some investigators and E-CCA by others [16, 28]. Second, although H69 cholangiocytes are considered non-malignant, they are SV40-transformed (i.e. immortalized) and therefore possess anti-apoptotic properties, and cannot be considered normal cholangiocytes. This distinction was apparent in their ability to form colonies/spheroids and their expression of certain SCSMs. Finally, future *in vivo* studies are required to compare the relative contributions of tumor cells and the microenvironment to tumor growth. Such experimentation is also required to identify the specific features within the tumor microenvironment responsible for any differences observed.

In conclusion, while cell proliferation and invasion are significantly increased in I-CCA compared to E-CCA cells, other tumor cell properties are similar in the two cell populations. In addition, the prevalence and SCSM expression profiles of CSCs within I-CCA and E-CCA cells are similar and do not associate with specific tumor cell growth features. Overall, these findings contribute to our

Table 2. P-values of correlations between stem cell surface markers and tumor growth features in cholangiocarcinoma cells

	Cell proliferation	Spheroid size	Colony formation	Cell migration	Cell invasion
CD13	0.4389634	0.3626529	0.4700548	0.09415884	0.8848501
CD24	0.9160627	0.8638522	0.05399868	0.7914219	0.954834
CD44	0.3972887	0.4706831	0.206752	0.4406875	0.8530665
CD90	0.7874514	0.4746822	0.4577624	0.6899347	0.8429261
EpCAM	0.5195574	0.3843364	0.4931796	0.2538196	0.1502015

understanding of the differences in the clinical courses of I-CCA and E-CCA in humans.

Funding source

Canadian Liver Foundation and Morberg Family Chair in Hepatology.

Disclosure

The authors declare no conflict of interest.

References

1. Bridgewater J, Galle PR, Khan SA, et al. Guidelines for the diagnosis and management of intrahepatic cholangiocarcinoma. J Hepatol 2014; 60: 1268-1289.
2. Blechacz B, Komuta M, Roskams T, et al. Clinical diagnosis and staging of cholangiocarcinoma. Nat Rev Gastroenterol Hepatol 2011; 8: 512-522.
3. Cardinale V, Carpino G, Reid L, et al. Multiple cells of origin in cholangiocarcinoma underlie biological, epidemiological and clinical heterogeneity. World J Gastrointest Oncol 2012; 4: 94-102.
4. Komuta M, Govaere O, Vandecaveye V, et al. Histological diversity in cholangiocellular carcinoma reflects the different cholangiocyte phenotypes. Hepatology 2012; 55: 1876-1888.
5. Aishima S, Oda Y. Pathogenesis and classification of intrahepatic cholangiocarcinoma: different characters of perihilar large duct type versus peripheral small duct type. J Hepatobiliary Pancreat Sci 2015; 22: 94-100.
6. Batlle E, Clevers H. Cancer stem cells revisited. Nat Med 2017; 23: 1124-1134.
7. Haraguchi N, Ishii H, Mimori K, et al. CD13 is a therapeutic target in human liver cancer stem cells. J Clin Invest 2010; 120: 3326-3339.
8. Keeratichamroen S, Leelawat K, Thongtawee T, et al. Expression of CD24 in cholangiocarcinoma cells is associated with disease progression and reduced patient survival. Int J Oncol 2011; 39: 873-881.
9. Gu MJ, Choi JH. Epithelial-mesenchymal transition phenotypes are associated with patient survival in intrahepatic cholangiocarcinoma. J Clin Pathol 2014; 67: 229-234.
10. Gu MJ, Jang BI. Clinicopathologic significance of Sox2, CD44 and CD44v6 expression in intrahepatic cholangiocarcinoma. Pathol Oncol Res 2014; 20: 655-660.
11. Leelawat K, Thongtawee T, Narong S, et al. Strong expression of CD133 is associated with increased cholangiocarcinoma progression. World J Gastroenterol 2011; 17: 1192-1198.
12. Yang J, Gong Y, Sontag DP, et al. Effects of low-density lipoprotein docosahexaenoic acid nanoparticles on cancer stem cells isolated from human hepatoma cell lines. Mol Biol Rep 2018; 45: 1023-1036.
13. Yamashita T, Wang XW. Cancer stem cells in the development of liver cancer. J Clin Invest 2013; 123: 1911-1918.
14. Peitzsch C, Tyutyunnykova A, Pantel K, et al. Cancer stem cells: The root of tumor recurrence and metastases. Semin Cancer Biol 2017; 44: 10-24.
15. Saijyo S, Kudo T, Suzuki M, et al. Establishment of a new extrahepatic bile duct carcinoma cell line, TFK-1. Tohoku J Exp Med 1995; 177: 61-71.
16. Meng F, DeMorrow S, Venter J, et al. Overexpression of membrane metalloendopeptidase inhibits substance P stimulation of cholangiocarcinoma growth. Am J Physiol Gastrointest Liver Physiol 2014; 306: G759-768.
17. Grubman SA, Perrone RD, Lee DW, et al. Regulation of intracellular pH by immortalized human intrahepatic biliary epithelial cell lines. Am J Physiol 1994; 266 (6 Pt 1): G1060-1070.
18. Borowicz S, Van Scoyk M, Avasarala S, et al. The soft agar colony formation assay. J Vis Exp 2014: e51998.
19. Guzman C, Bagga M, Kaur A, et al. ColonyArea: an ImageJ plugin to automatically quantify colony formation in clonogenic assays. PloS One 2014; 9: e92444.
20. Ruster B, Grace B, Seitz O, et al. Induction and detection of human mesenchymal stem cell migration in the 48-well reusable transwell assay. Stem Cells Dev 2005; 14: 231-235.
21. Nakanuma Y, Sato Y. Cystic and papillary neoplasm involving peribiliary glands: a biliary counterpart of branch-type intraductal papillary mucinous [corrected] neoplasm? Hepatology 2012; 55: 2040-2041.
22. Bragazzi MC, Ridola L, Safarikia S, et al. New insights into cholangiocarcinoma: multiple stems and related cell lineages of origin. Ann Gastroenterol 2018; 31: 42-55.
23. Cardinale V, Bragazzi MC, Carpino G, et al. Cholangiocarcinoma: increasing burden of classifications. Hepatobiliary Surg Nutr 2013; 2: 272-280.
24. Pallini R, Ricci-Vitiani L, Banna GL, et al. Cancer stem cell analysis and clinical outcome in patients with glioblastoma multiforme. Clin Cancer Res 2008; 14: 8205-8212.
25. Cardinale V, Renzi A, Carpino G, et al. Profiles of cancer stem cell subpopulations in cholangiocarcinomas. Am J Pathol 2015; 185: 1724-1739.
26. Leyva-Illades D, McMillin M, Quinn M, et al. Cholangiocarcinoma pathogenesis: Role of the tumor microenvironment. Transl Gastrointest Cancer 2012; 1: 71-80.
27. Sombattheera S, Proungvitaya T, Limpaiboon T, et al. Total serum bile acid as a potential marker for the diagnosis of cholangiocarcinoma without jaundice. Asian Pac J Cancer Prev 2015; 16: 1367-1370.
28. Shimizu T, Yokomuro S, Mizuguchi Y, et al. Effect of transforming growth factor-beta1 on human intrahepatic cholangiocarcinoma cell growth. World J Gastroenterol 2006; 12: 6316-6324.